united nations educational, scientific and cultural organization

international atomic energy agency

the
abdus salam
international centre for theoretical physics

SMR 1232 - 32

XII WORKSHOP ON
STRONGLY CORRELATED ELECTRON SYSTEMS

17 - 28 July 2000

QUANTUM DOT

L.I. GLAZMAN
University of Minnesota
55455 Minneapolis, USA

These are preliminary lecture notes, intended only for distribution to participants.

QUANTUM DOT

(Many-body physics of quantum dots)

L.I. Glazman
University of Minnesota

ICTP Trieste
July 25, 2000

Outline

1. Early observations of charge discreteness in tunneling

2. What is a quantum dot

3. Coulomb blockade of conduction through a dot

4. Interference effects: Mesoscopic fluctutations of the conductance

5. Spin of a quantum dot and the Kondo effect

Millikan oil-drop experiment, 1909

(R.A. Millikan, Phys. Rev. 32, 349 (1911))

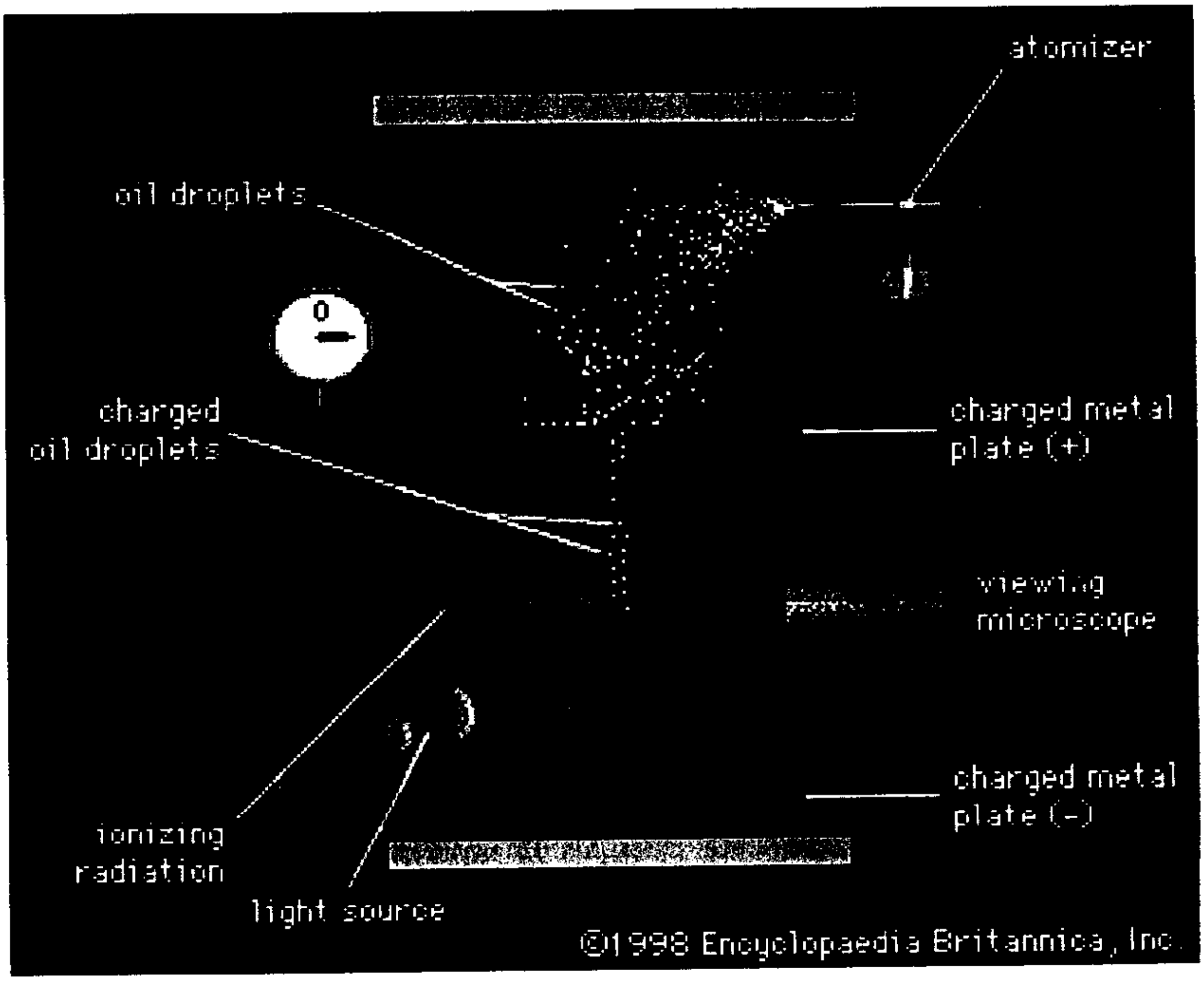

Indirect evidence of charging effects:

C. J. Gorter, Physica 17, 777 (1951)

C. A. Neugebauer, M. B. Webb, J. Appl. Phys. 33, 74 (1962

hopping (in-plane conductivity) in granular films

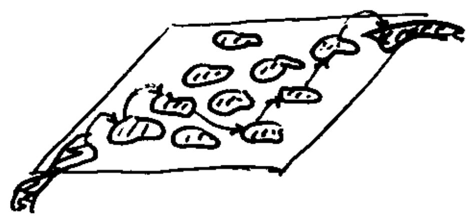

Clear demonstration of the role of charging: "vertical" tunneling through a layer of grains:

I. Giaever, H. R. Zeller, PRL 20, 1504 (68), Phys. Rev (1969

J. Lambe, R. C. Jaklevic, PRL 22, 1371 (1969)

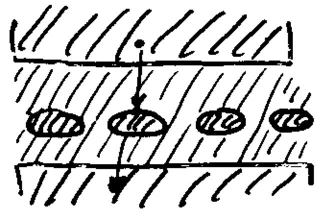

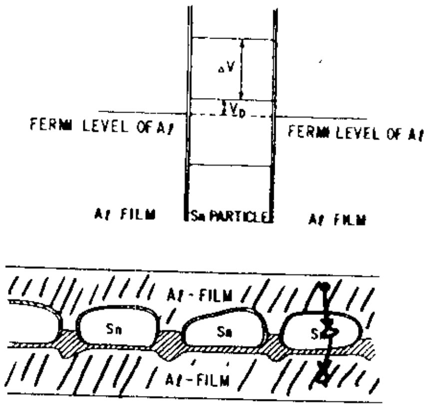

FIG. 1. Model and level scheme of Sn particles in a tunnel junction. V_D is the energy in eV of the last filled state at $T=0$ of the Sn particle, with respect to the Fermi energy of Al. $\Delta V = e/C$ is the voltage change of the particle caused by addition of one electron. In equilibrium $-e/2C \geq V_D \geq e/2C$ holds.

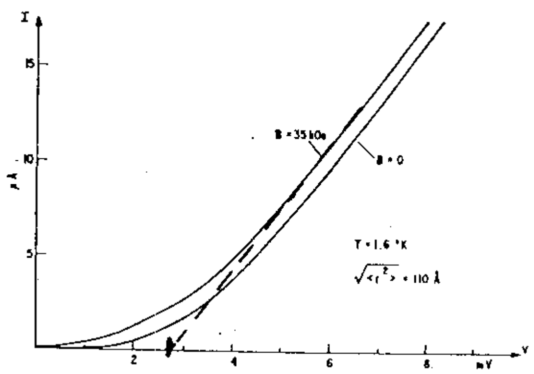

FIG. 7. Current-versus-voltage characteristic of a junction with average particle radius $r=110$ Å at 1.6°K for $H=0$ (particles superconducting) and $H=35$ kOe (particles normal).

$$\Delta E_N = \frac{(N+1)^2 e^2}{2C} - \frac{N^2 e^2}{2C}$$

$$= \frac{2N+1}{2C} e^2$$

$$eV^{(N)}_{APPL} \simeq \Delta E_N = (2N+1) \cdot \frac{e^2}{2C}$$

When a voltage is applied we get a current flow through the junction. The electrons can flow from one side of the junction to the other by essentially three different mechanisms:

(1) direct tunneling through the aluminum oxide, avoiding the Sn particles. This mechanism gives a constant, voltage- and temperature-independent, background conductivity. For properly prepared junctions with a particle radius $r > 30$ Å direct tunneling can be made completely negligible even at 1°K and at zero bias.

(2) tunneling from one Al film onto a Sn particle, localizing the electron there and then in turn tunneling out on to the other side. This process needs an activation energy which in turn is responsible for the zero-bias resistance peak. We will discuss this process in most of the remainder of the paper.

(3) tunneling from one aluminum film through a particle and out onto the other aluminum film without actually localizing the electron on the particle. The particle is only involved as an intermediate state; thus, the process is of second order. This process can conceivably become important at low temperatures and at low voltages; however, no experimental evidence has been found for this process. It is very similar in principle to Anderson's model[18] for tunneling involving intermediate magnetic impurity states.

According to process (2), in order to get a current flow the number of electrons on a Sn particle has to be changed by at least one. The activation energy required is equal to the difference of the Coulomb energies in the initial and the final state, i.e.,

$$E = \tfrac{1}{2}(e/C \pm V_D)^2 C - \tfrac{1}{2} V_D^2 C, \tag{1}$$

where the positive sign holds for adding an electron and the negative sign for subtracting an electron. This activation energy can only be supplied by the battery. We would like to emphasize again that E is a pure classical Coulomb energy, and that all effects due to the level spacing in the particle have been neglected since the level spacing is small compared with E.

The capacitance of a specific particle, C, is simply the sum of the capacitance between the particle and the

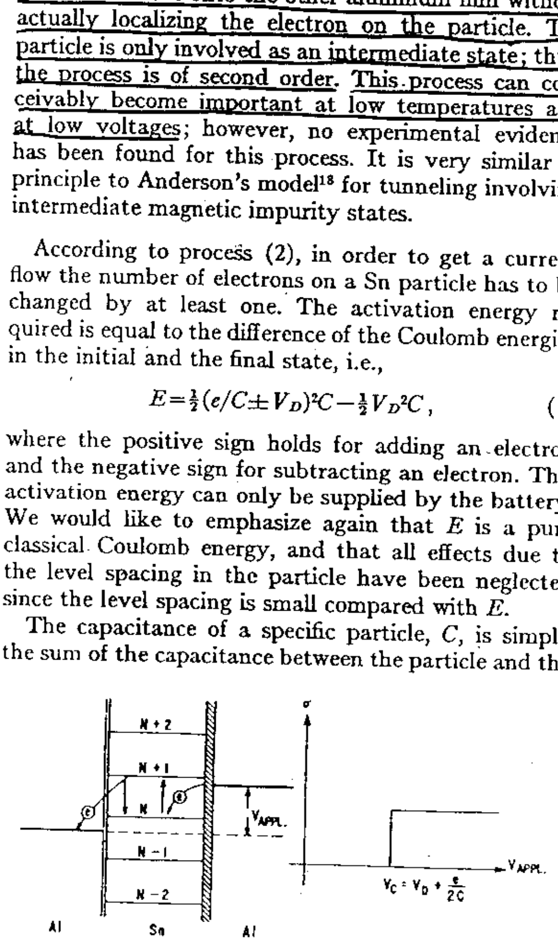

FIG. 13. Mechanism of current flow for an asymmetric junction ($C_L \gg C_R$). An electron from the right film tunnels into the particle, raising its electron number from N to $N+1$ and its voltage from V_D to $V_D + e/C$. In a next step the electron tunnels out onto the left film bringing the particle back in its ground state. This results in a step function for the conductivity as a function of voltage.

- Theory
  (kinetic equations + charge discreteness):
  R.I. Shekhter, JETP **36**, 747 (1973);
  I.O. Kulik, R.I. Shekhter, **41**, 308 (1975).

  "Orthodox theory of Coulomb blockade":
  Reduces *e-e* interaction to the charging effect, energy $E_C = e^2/C$, and treats tunneling as *sequential* events (no coherence).

- Gate-controlled single-charge tunneling,
  single-electron transistor:
  T.A. Fulton, G.J. Dolan, PRL **59**, 109 (1987) - experiment

Observation of Single-Electron Charging Effects in Small Tunnel Junctions

T. A. Fulton and G. J. Dolan
AT&T Bell Laboratories, Murray Hill, New Jersey 07974
(Received 6 March 1987)

Unusual structure and large electric-field-induced oscillations have been observed in the current-voltage curves of small-area tunnel junctions arranged in a low-capacitance ($\lesssim 1$ fF) multiple-junction configuration. This behavior arises from the tunneling of individual electrons charging and discharging the capacitance. The observations are in accord with what would be expected from a simple model of the charging energies and voltage fluctuations of e/C associated with such effects.

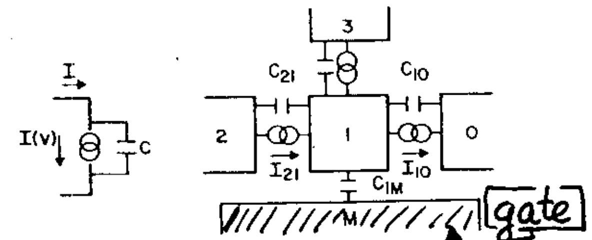

FIG. 1. Left: An equivalent circuit for discussion of charging effects for a single junction. Right: A comparable triple-junction circuit model.

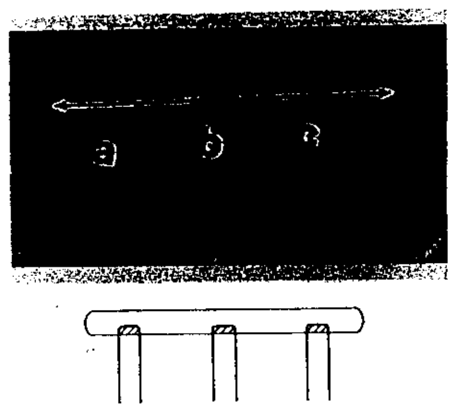

FIG. 2. A scanning-electron micrograph of a typical sample. Junctions labeled a, b, and c are formed where the vertical electrodes overlap and contact the longer horizontal central electrode. The bar is 1 μm long. The configuration is also shown in the accompanying drawing.

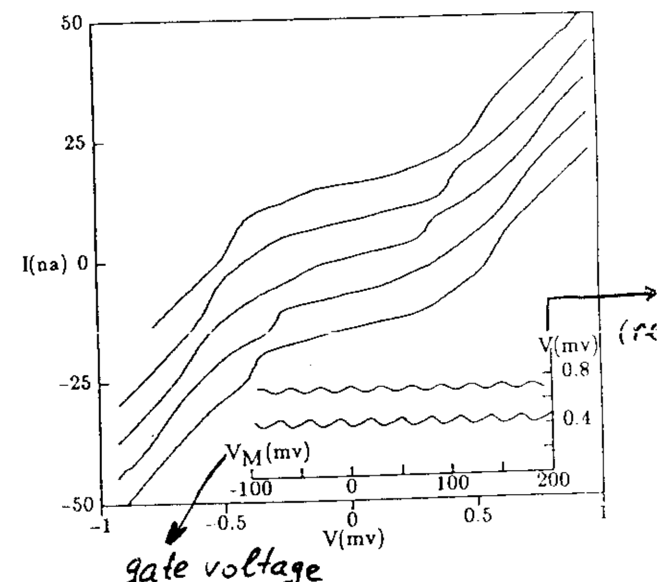

FIG. 5. I-V curves for a sample at $T=1.1$ K for a set of equally spaced substrate biases covering $\frac{5}{6}$ of a cycle. Curves are offset by increments of 7.5 nA. Inset: V vs V_M for two fixed currents $I=10.5$ and 26 nA.

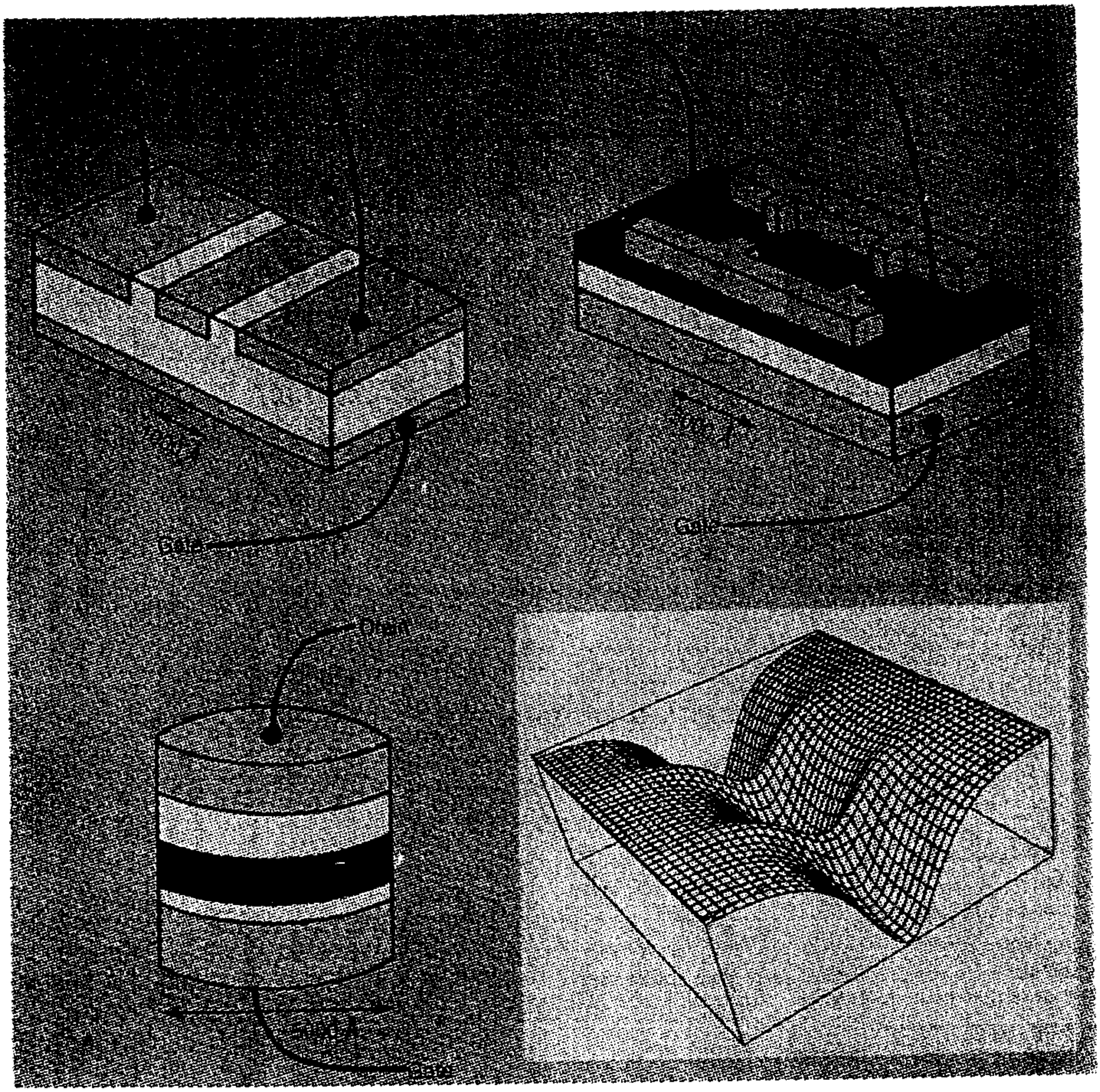

M. Kastner, Physics Today, Jan. 93, p. 24

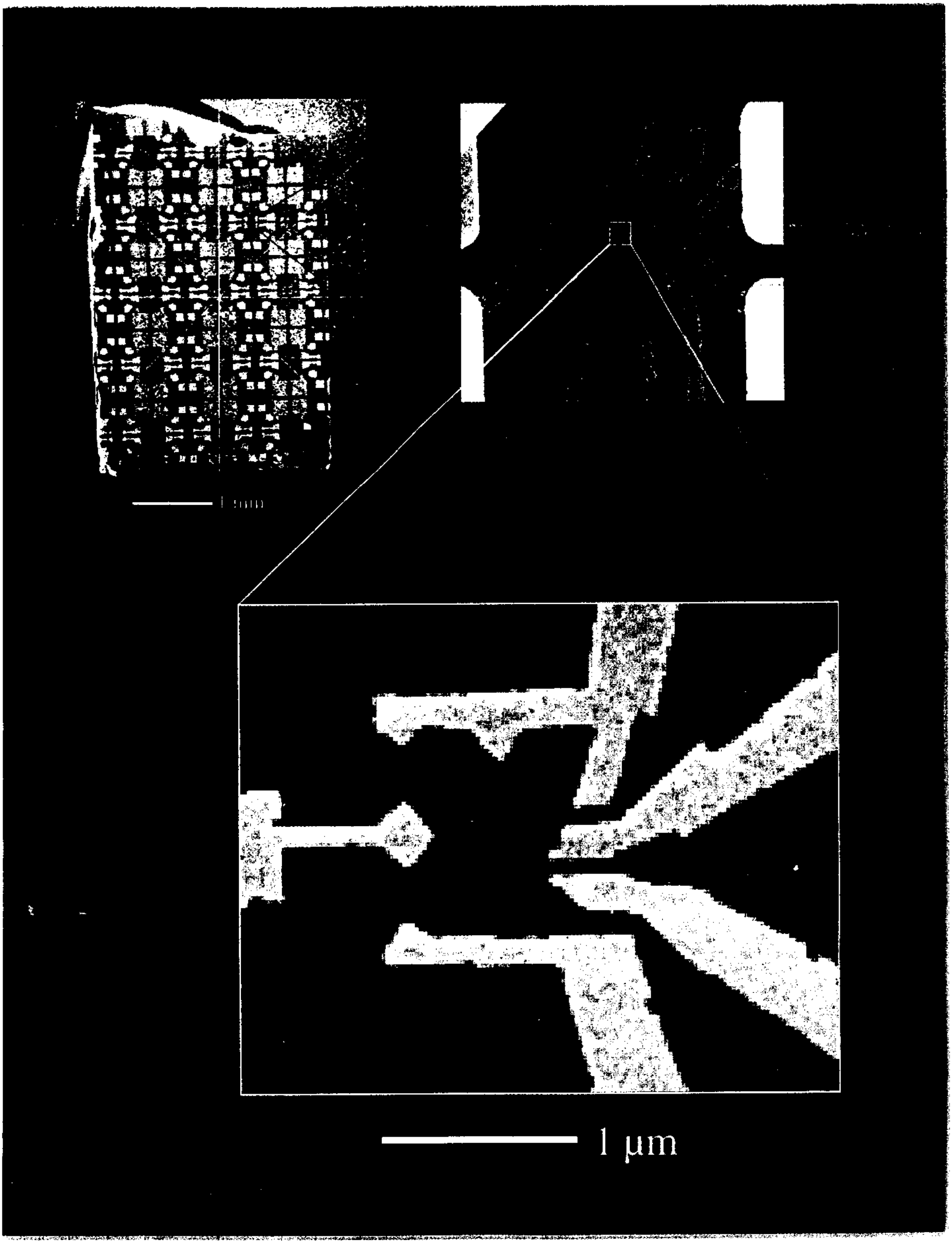
1 mm
1 μm

Quantum dot $\equiv$ mesoscopic puddle of electron <u>liquid</u>

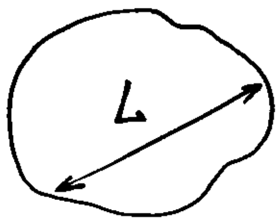

$\underline{L \gg \lambda_F}$

* Dominant energy scale: charging

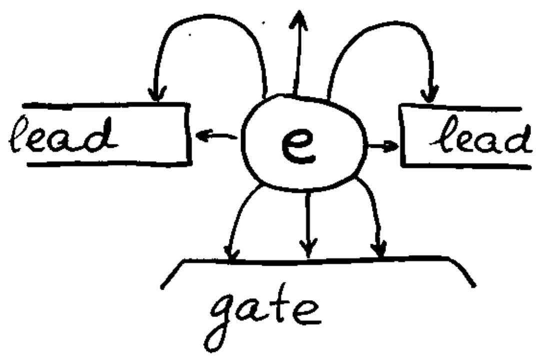

$$E_c = \frac{e^2}{2C}, \qquad C \sim L$$

* Smaller energy scale: discrete level spacing

$$\delta E = \frac{1}{\nu L^d}$$

$$\underline{\frac{\delta E}{E_c}} = \frac{\hbar v_F}{e^2} \cdot \left(\frac{\lambda_F}{L}\right)^{d-1} \simeq \underline{\frac{1}{r_s} \cdot \left(\frac{\lambda_F}{L}\right)^{d-1} \ll 1}$$

($d \equiv$ dimension)

Charge of a quantum dot

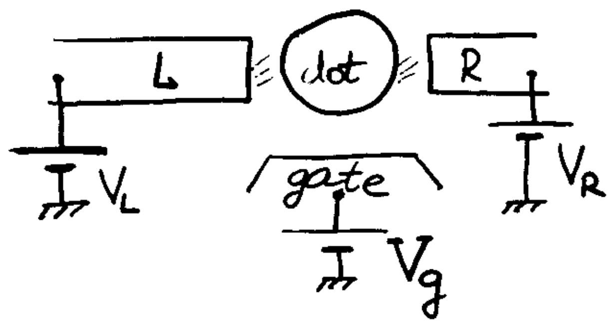

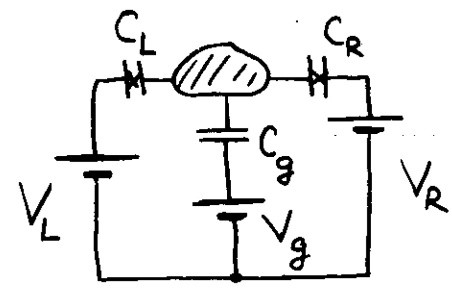

Electrostatic energy: $E(\hat{N}) = E_c \cdot (\hat{N} - \mathcal{N})^2$,

$$\mathcal{N} \equiv V_g / eC_g$$

min $[E(N)]$: $N = \mathcal{N}$ for <u>continuous</u> N

Discrete N: <u>staircase</u>

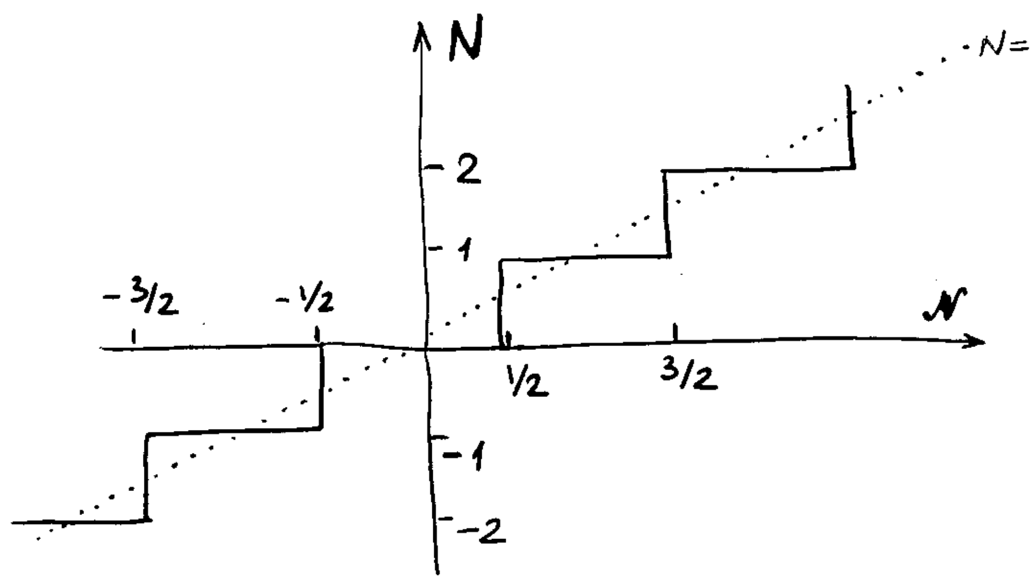

Characteristic temperature: E_c.

At $T \ll E_c$, and assuming $\delta E \to 0$

$$G(\mathcal{N}, T) = \frac{1}{2R_\infty} \cdot \frac{E_c(\mathcal{N}-\mathcal{N}^*)/T}{\sinh[E_c(\mathcal{N}-\mathcal{N}^*)/T]} \quad , \quad \mathcal{N} \equiv \frac{V_g}{eC_g}$$

$$\mathcal{N}^* \equiv n + \tfrac{1}{2}$$

(L.G., Shekhter 1989)

R_∞ – "usual" high-T value of resistance for two tunnel junctions in series:

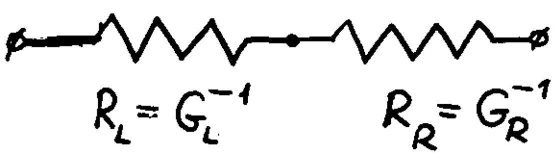

$$R_\infty = R_L + R_R = \frac{G_L + G_R}{G_L G_R}$$

In the limit $T \to 0$ conductance $G(\mathcal{N}, T) \to 0$ exponentially at all $\mathcal{N}$ except isolated points of charge degeneracy $\mathcal{N}^* \equiv n + \frac{1}{2}$

In the continuous spectrum approx.,
all peaks have the <u>same</u> amplitude, $G_{max} = \frac{1}{2R}$

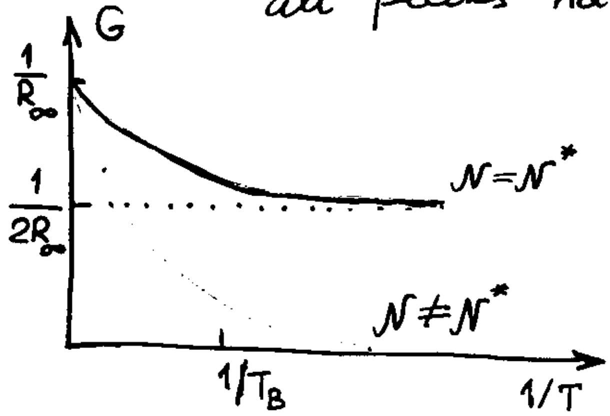

(e-like or h-like degeneracy)

Strong Tunneling in the Single-Electron Transistor

P. Joyez, V. Bouchiat, D. Esteve, C. Urbina, and M. H. Devoret
Service de Physique de l'Etat Condensé, Commissariat à l'Energie Atomique, Saclay, 91191 Gif-sur-Yvette, France
(Received 27 January 1997)

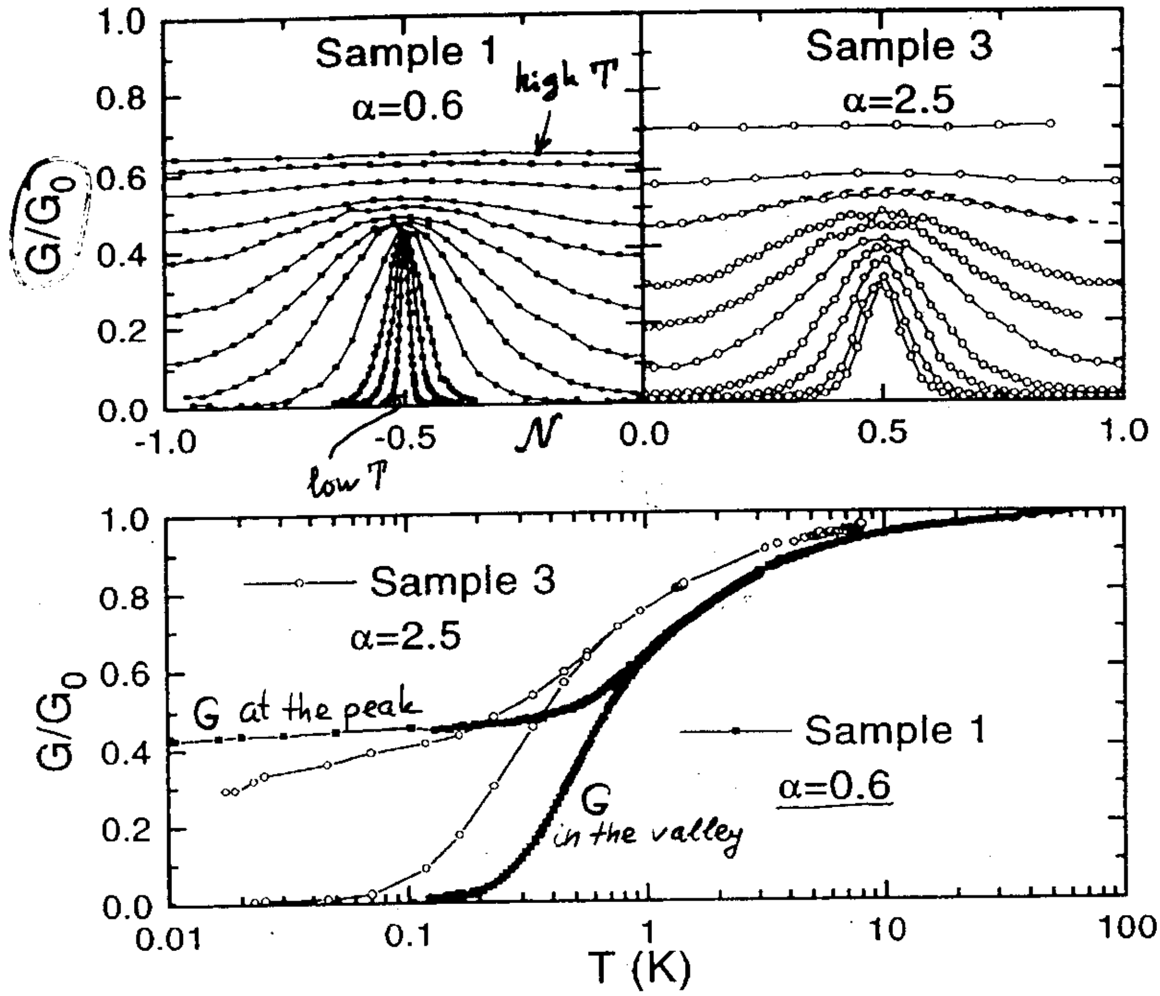

$$\delta E \ll E_c = \frac{e^2}{2C}$$

Even smaller energy scale: <u>width</u> of an individual <u>discrete</u> <u>level</u> Γ.

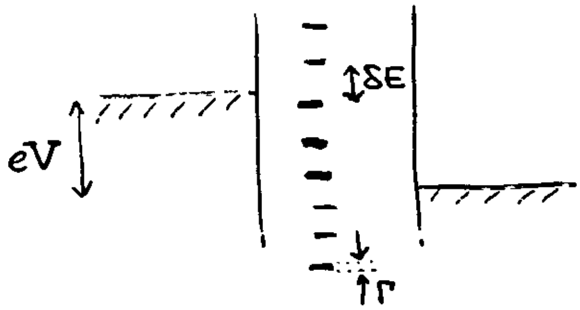

$$\frac{h}{\Gamma} = \tau_{dw}, \text{ dwelling time}$$

$$I \sim \frac{e}{\tau_{dw}} \cdot 2 \cdot \frac{eV}{\delta E} \sim 2\frac{e^2}{h}\frac{\Gamma}{\delta E} \cdot V$$

$$G = \frac{I}{V} \quad \Rightarrow \quad \boxed{G \simeq \frac{2e^2}{h}\frac{\Gamma}{\delta E}}$$

$$G \ll \frac{e^2}{h} \quad \Rightarrow \quad \Gamma \ll \delta E$$

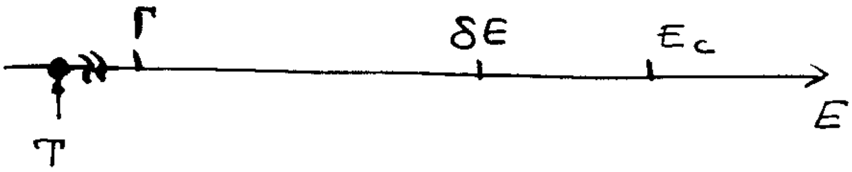

Many-body correlations between the dot and electrons in the leads may become important (due to the electron spin)

T<<Γ

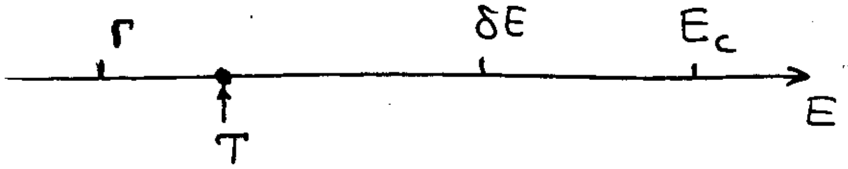

In resonances, the conduction occurs via separate discrete levels of the dot.

Statistical properties of the wavefunctions in the dot become important

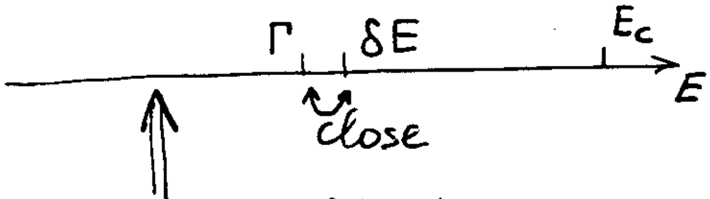

mesoscopic fluctuations of <u>many</u> - <u>body</u> <u>states</u>

$G \simeq \frac{2e^2}{h}$, charge is <u>**not**</u> quantized;

"mixed valence regime

Fluctuations of conductance through a quantum dot

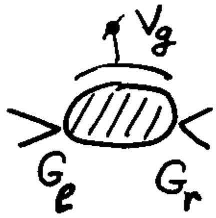

$$G_\ell\,,\,G_r \ll \frac{e^2}{h}$$

$$G = \frac{e^2}{\pi\hbar}\int d\varepsilon\, T(\varepsilon)\frac{\partial f}{\partial \varepsilon}$$

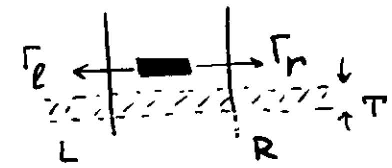

Low temperatures ($T \lesssim \delta E$) $\Rightarrow$ narrow peaks in the conductance,

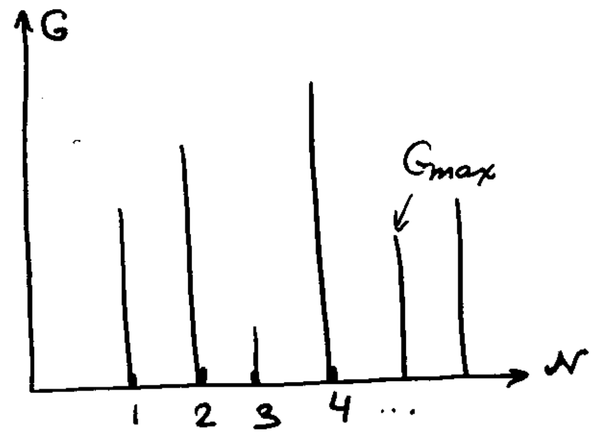

$$G_{max} = \frac{e^2}{4h}\,\frac{\Gamma_\ell\Gamma_r}{(\Gamma_\ell+\Gamma_r)T} \equiv \frac{e^2}{4hT}\cdot\Gamma$$

$$\langle \Gamma_i \rangle = \frac{\hbar}{e^2}\,G_i \cdot 2\,\delta E$$

but: $\Gamma_i \propto |\psi_n(R_i)|^2$,

and <u>fluctuates</u> (Porter-Thomas, 1956)

$$P(\Gamma) = \int d\Gamma_\ell\, d\Gamma_r\; P_{PT}(\Gamma_\ell)\, P_{PT}(\Gamma_r)\,\delta\!\left(\frac{\Gamma_\ell\Gamma_r}{\Gamma_\ell+\Gamma_r} - \Gamma\right)$$

Porter-Thomas distribution for neutron widths Γ

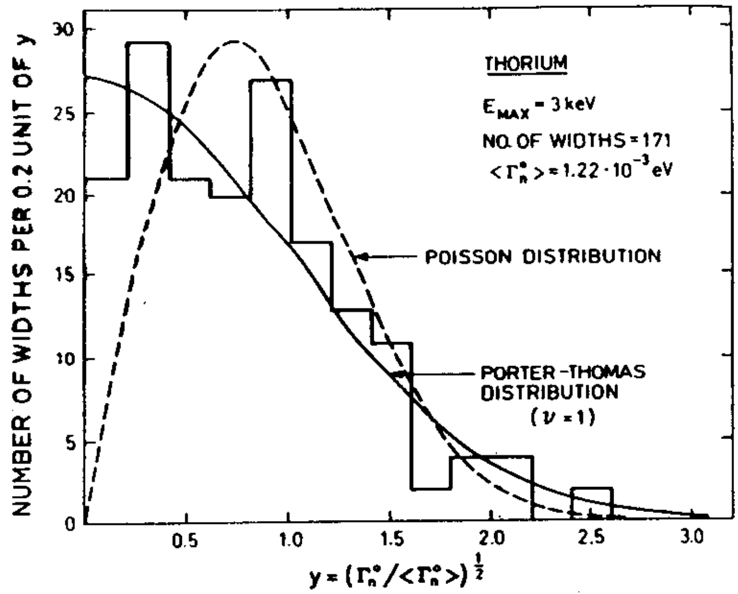

Figure 2-10 The figure plots the probability distribution of the reduced neutron widths observed in the reaction $n + {}^{232}\mathrm{Th}$ ($\Gamma_n^{(0)}(E_r) = \Gamma_n(E_r)E_r^{-1/2}$(eV)). The data are taken from J. B. Garg, J. Rainwater, J. S. Petersen, and W. W. Havens, Jr., *Phys. Rev.* 134, B985 (1964).

▼ The theoretical distribution obtained in the limit of extreme configuration mixing (Porter and Thomas, 1956) is a χ^2 distribution with $\nu = 1$. Since such a distribution varies as $(\Gamma_n^{(0)})^{-1/2}$ for small values of $\Gamma_n^{(0)}$ (see Eq. (2C-28)),

$$P(\Gamma_n^{(0)}) = (2\pi\Gamma_n^{(0)}\langle\Gamma_n^{(0)}\rangle)^{-1/2}\exp\left\{-\frac{\Gamma_n^{(0)}}{2\langle\Gamma_n^{(0)}\rangle}\right\} \tag{2-115}$$

it is convenient to plot the distribution of $(\Gamma_n^{(0)})^{1/2}$. The observed widths in Fig. 2-10 follow the distribution (2-115) rather well, but are in disagreement with the Poisson distribution (a χ^2 distribution with $\nu = 2$; see Eq. (2C-29)).

Compound nucleus state $\equiv$ (normalized) random vector of large dimension

Neutron width $\propto$ square of one component of this vector

$$P(c_1, \ldots, c_N) = \frac{2}{\Omega_N}\,\delta\Big(1 - \sum_{i=1}^{N} c_i^2\Big), \qquad \Omega_N = \frac{N\pi^{N/2}}{\Gamma(\frac{N}{2}+1)}$$

$$P(c_1) \simeq \sqrt{\frac{N}{2\pi}}\,\exp\Big\{-\frac{N}{2}c_1^2\Big\} \qquad P(c)\,dc = \frac{1}{2c}P(c^2)\,dc^2$$

$$P_{PT}(\Gamma) \propto P(c_1^2) \propto \frac{1}{\langle c_1^2\rangle^{1/4} c_1^{1/2}}\exp\Big\{-\frac{c_1^2}{2\langle c_1^2\rangle}\Big\} \qquad (\mathrm{GOE})$$

Non-Gaussian Distribution of Coulomb Blockade Peak Heights in Quantum Dots

A. M. Chang,[1] H. U. Baranger,[1] L. N. Pfeiffer,[1] K. W. West,[1] and T. Y. Chang[2]
[1]*AT&T Bell Laboratories, 600 Mountain Avenue, Murray Hill, New Jersey 07974-0636*
[2]*AT&T Bell Laboratories, Crawfords Corner Road, Holmdel, New Jersey 07733*
(Received 26 July 1995)

We have observed a strongly non-Gaussian distribution of Coulomb blockade conductance peak heights for tunneling through quantum dots. At zero magnetic field, a low-conductance spike dominates the distribution; the distribution at nonzero field is distinctly different and still non-Gaussian. The observed distributions are consistent with theoretical predictions based on single-level tunneling and the concept of "quantum chaos" in a closed system weakly coupled to leads.

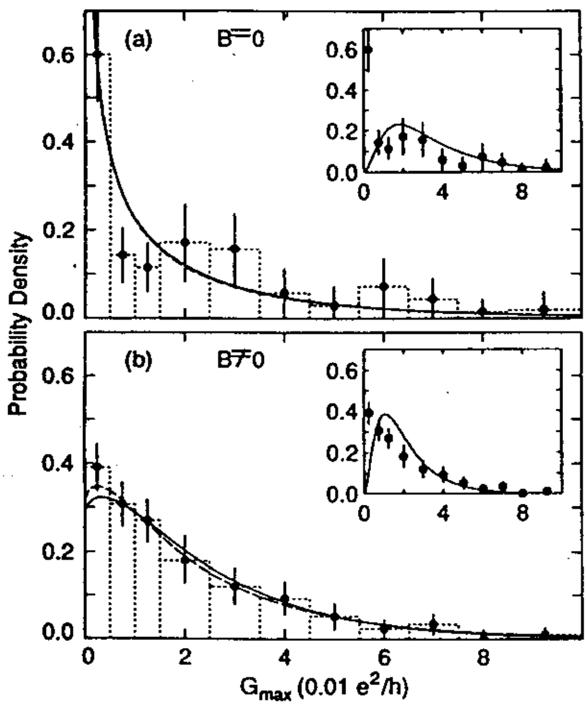

FIG. 4. Histograms of conductance peak heights for (a) $B = 0$ and (b) $B \neq 0$. Data are scaled to unit area; there are 72 peaks for $B = 0$ and 216 peaks for $B \neq 0$; the statistical error bars are generated by bootstrap resampling. Note the non-Gaussian shape of both distributions and the strong spike near zero in the $B = 0$ distribution. Fits to the data using both the fixed pincher theory (solid) and the theory averaged over pincher variation (dashed) are excellent. The insets show fits by $\chi_6^2(\alpha)$—a more Gaussian distribution—averaged over the pincher variation; the fit is extremely poor.

$$G_{max} = \frac{e^2}{h}\frac{\pi\bar{\Gamma}}{2kT}\alpha$$

$$P(\alpha) = \sqrt{\frac{2}{\pi\alpha}}\, e^{-2\alpha} \qquad \text{GOE } (B=0)$$

$$P(\alpha) = 4\alpha[K_0(2\alpha) + K_1(2\alpha)]e^{-2\alpha} \qquad \text{GUE } (B>B_c)$$

(Jalabert, Stone, Alhassid, 1992)

Multichannel case:
Mucciolo, Prigodin, Altshuler, 1995

Crossover GOE → GUE:
Falko, Efetov, 1996

Statistics and Parametric Correlations of Coulomb Blockade Peak Fluctuations in Quantum Dots

J. A. Folk, S. R. Patel, S. F. Godijn, A. G. Huibers, S. M. Cronenwett, and C. M. Marcus
Department of Physics, Stanford University, Stanford, California 94305-4060

K. Campman and A. C. Gossard
Materials Department, University of California at Santa Barbara, Santa Barbara, California 93106
(Received 18 September 1995)

We report measurements of mesoscopic fluctuations of Coulomb blockade peaks in a shape-deformable GaAs quantum dot. Distributions of peak heights agree with predicted universal functions for both zero and nonzero magnetic fields. Parametric fluctuations of peak height and position, measured using a two-dimensional sweep over gate voltage and magnetic field, yield autocorrelations of height fluctuations consistent with a predicted Lorentzian-squared form for the unitary ensemble. We discuss the dependence of the correlation field on temperature and coupling to the leads as the dot is opened.

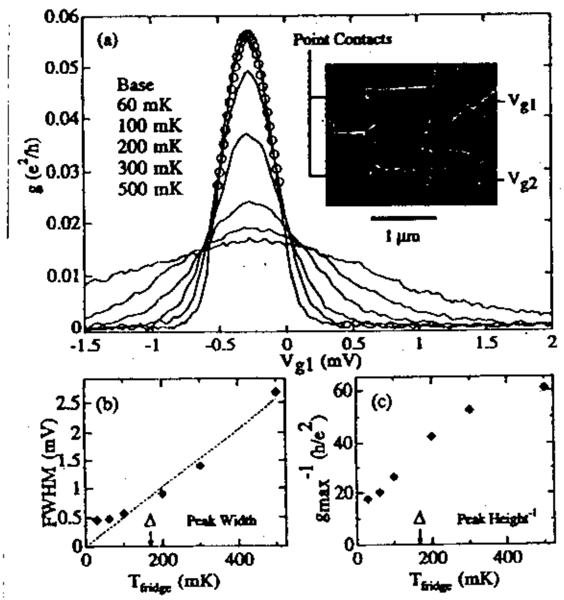

FIG. 1. (a) Temperature dependence of Coulomb peak line shape for the larger dot ($\Delta = 15\ \mu$eV). Circles show fit of base temperature peak by $g/g_{\max} = \cosh^{-2}(\eta eV_g/2kT)$. Inset: Micrograph of the larger dot. V_{g1} and V_{g2} are shape distorting gates. (b) Peak width measured as FWHM of the fit to $\cosh^{-2}$. Linear behavior at high temperatures gives voltage-to-energy scale $\eta = 0.12$. (c) Inverse peak height decreases with temperature for $kT < \Delta$. From saturations at low T in (b) and (c) we estimate the electron temperature in the dot to be 70 ± 20 mK.

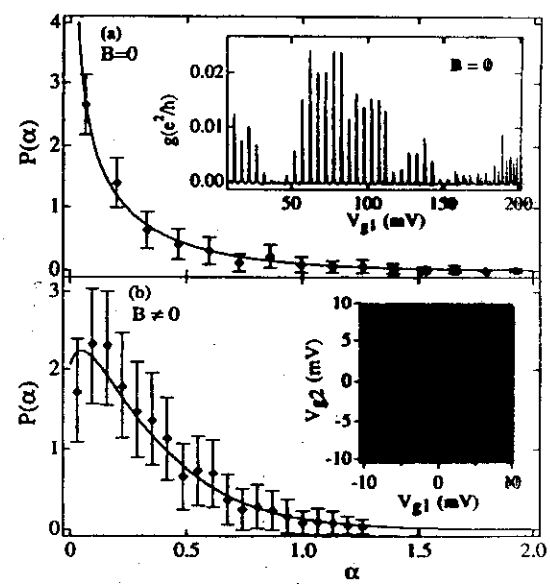

FIG. 2. Distribution of Coulomb peak conductances, scaled to dimensionless conductances α [Eq. (2)] for (a) the orthogonal ($B = 0$) ensemble and (b) the unitary ensemble ($B \neq 0$). Insets: (a) Example of a set of peaks from which the distribution was obtained. (b) Grayscale plot of small region of gate-gate sweep used to derive these distributions, showing Coulomb "ridges" along lines of constant area (lighter = higher conductance). Error bars assume ~90 statistically independent samples (see text).

19

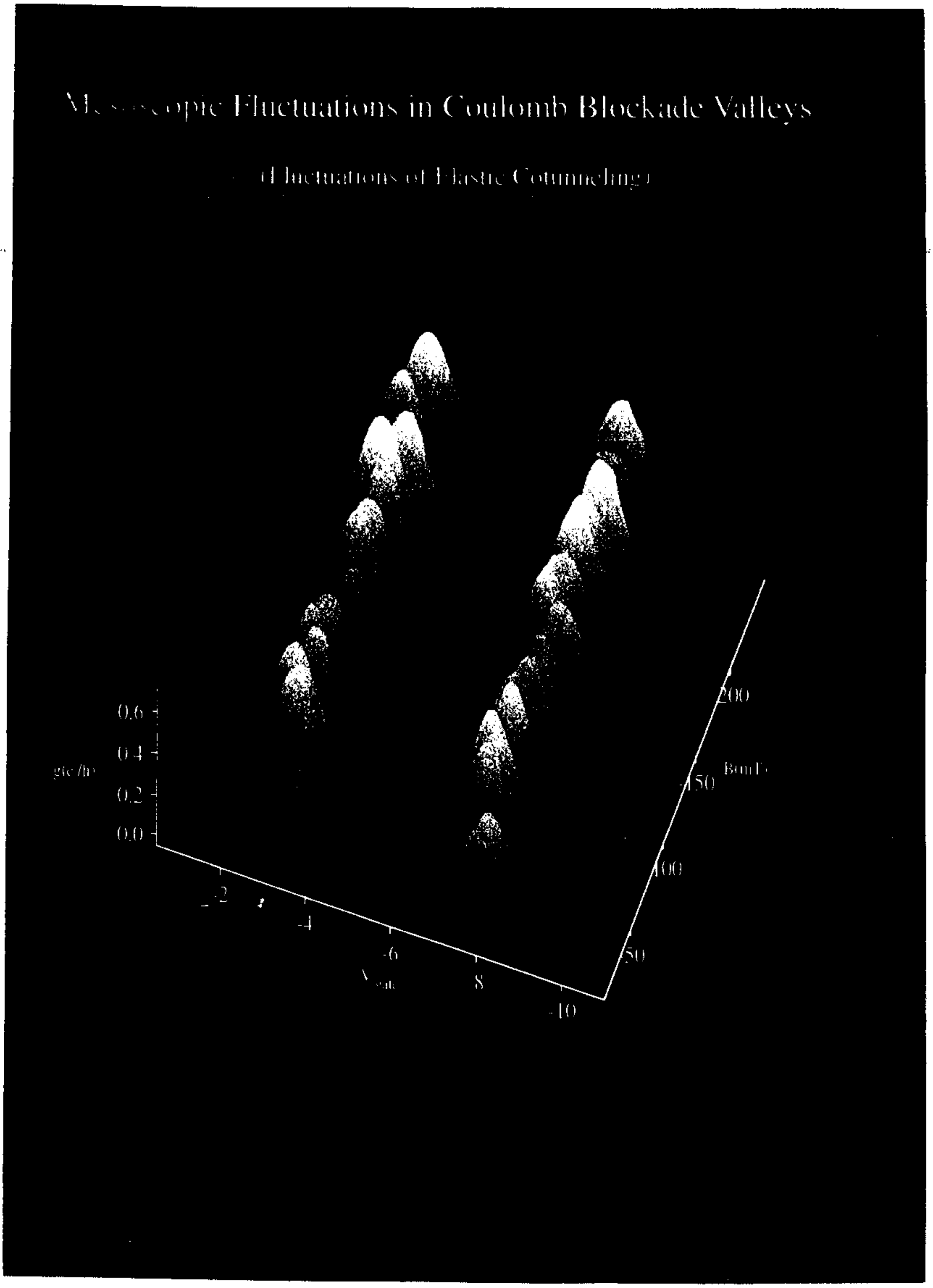
Fluctuations in Coulomb Blockade Valleys
(Fluctuations of Elastic Cotunneling)
0.6
0.4
0.2
0.0
-2
-4
-6
8
-10
50
100
150
200

Higher-order tunneling processes
(co-tunneling)

* Inelastic co-tunneling (Averin, Odintsov 88)

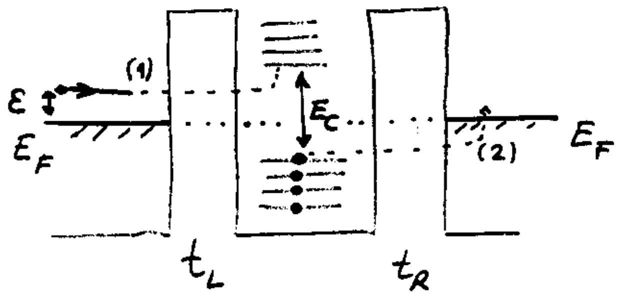

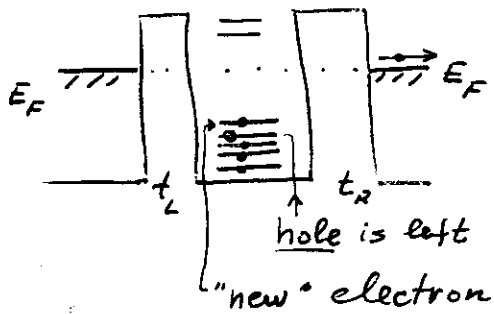

$$\delta E \ll \varepsilon \ll E_C$$

$$\left.\begin{array}{l} A_{in} \propto \dfrac{t_L t_R}{E_C} \\ \text{e-h phase space} \propto T^2 \end{array}\right\} \Rightarrow \quad \underline{\underline{G_{in}}} \propto |A_{in}|^2\, T^2 \sim \underline{\underline{\frac{G_L G_R}{e^2/h}\left(\frac{T}{E_C}\right)^2}}$$

$$G_{in} \gg G_{act.} \iff T \lesssim \frac{E_C}{\ln\left(\dfrac{e^2/h}{G_L+G_R}\right)}$$

* Elastic co-tunneling (Averin, Nazarov 91)

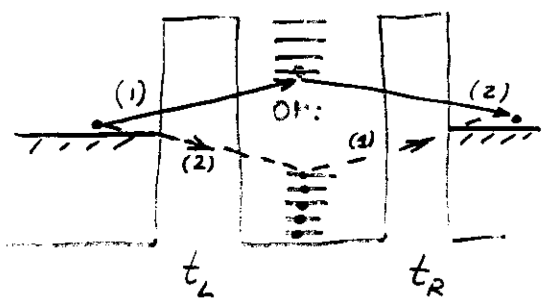

$$\underline{\underline{\langle G_{el}\rangle}} \sim \underline{\underline{\frac{G_L G_R}{e^2/h}\cdot\frac{\delta E}{E_C}}}$$

$$G_{el} \gtrsim G_{in} \iff T \lesssim \sqrt{E_C\,\delta E}$$

Fluctuations of G_{el}: Aleiner, L.G. (1996

Many contributions to the amplitude:

$$A = \sum_{i=1}^{N} A_i \,, \qquad N \sim \frac{E_c}{\delta E}$$

$$|A|^2 = \underbrace{\sum_{i=1}^{N} |A_i|^2}_{N \text{ terms}} + \underbrace{\sum_{i \neq j}^{N} A_i A_j^*}_{N^2 - N \text{ terms}}$$

$$\langle |A|^2 \rangle \propto N \langle |A_i|^2 \rangle$$

$$\underline{\mathrm{var}\, |A|^2} \propto \sqrt{N^2 - N} \sim \underline{\langle |A|^2 \rangle}$$

$$\langle |A_i|^2 \rangle \sim \frac{\Gamma_L \Gamma_R}{E_c^2} \sim \frac{h}{e^2} G_L G_R \left(\frac{\delta E}{E_c} \right)^2$$

Elastic co-tunneling

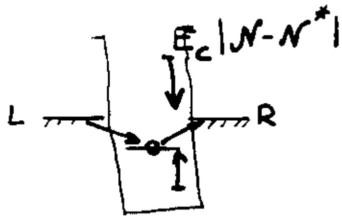

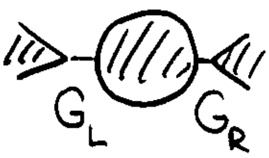

$$\langle G_{el} \rangle \sim \frac{h}{e^2} G_L G_R \cdot \frac{\delta E}{E_c} \cdot \frac{1}{|\mathcal{N}-\mathcal{N}^*|}$$

$$\mathcal{N}^* = n + \frac{1}{2}$$

Fluctuations of G_{el} :

$$\langle \delta G(B_1)\, \delta G(B_2) \rangle = \langle G_{el} \rangle^2 \cdot F\left(\frac{|B_1 - B_2|}{B_c} \right)$$

Aleiner, L.G. PRL 77, 2057 (1996)

Characteristic field

$$B_c \sim \frac{\Phi_0}{S} \sqrt{\frac{E_c}{E_T} |\mathcal{N}-\mathcal{N}^*|}$$

$$\frac{1}{2} \gtrsim |\mathcal{N}-\mathcal{N}^*| \gtrsim \frac{\delta E}{E_c}$$

$E_T \sim \frac{\hbar D}{S}$: Thouless energy

B_c depends on the gate voltage:

$\min G \leftrightarrow \max B_c$

OSCILLATION OF B_c – OUT OF PHASE WITH $\langle G \rangle$

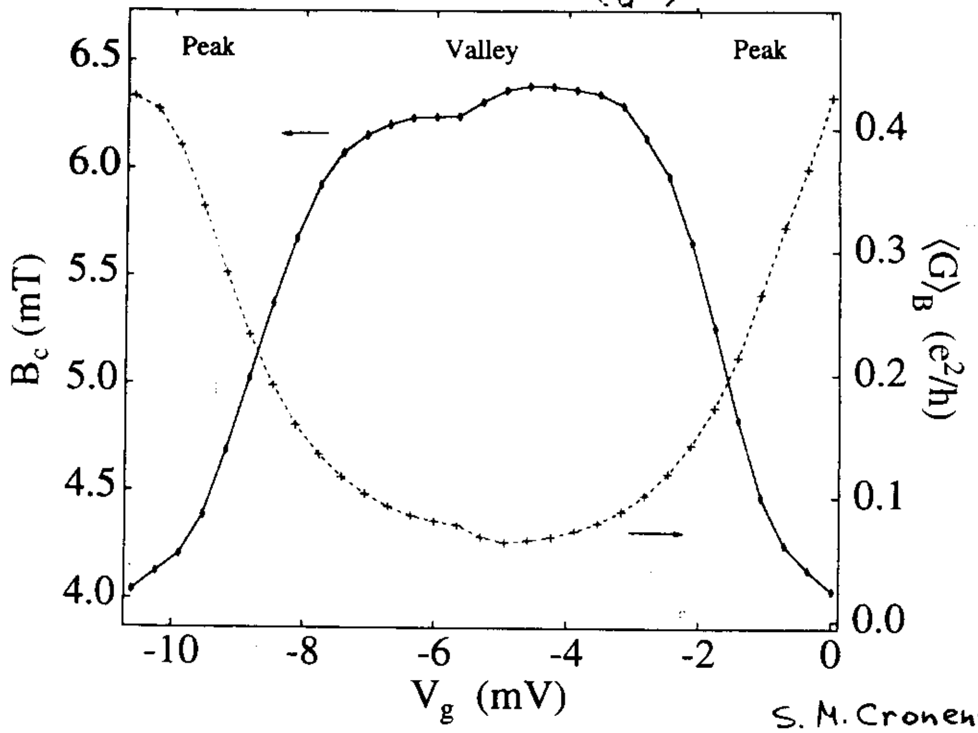

S. M. Cronenwet et. al
(C.M. Marcus, Stanford)
PRL $\underline{79}$ 2312 (1997)

$B_c = k \frac{\phi_0}{A} \sqrt{\frac{E_L}{E_T}}$

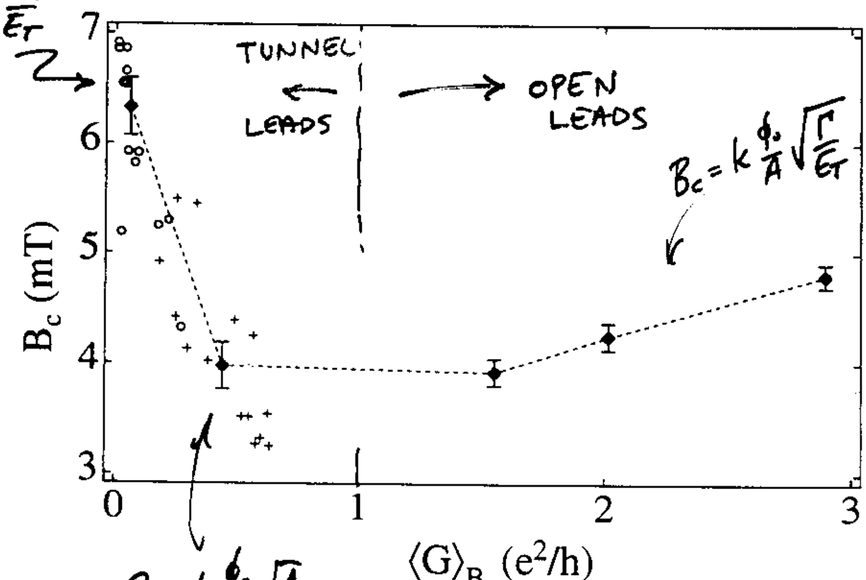

$B_c = k \frac{\phi_0}{A} \sqrt{\frac{\Delta}{E_T}}$

Kondo Conductance

(Odd N, small r_s)

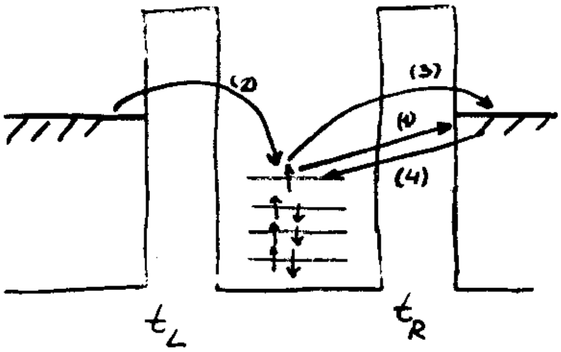

Starts with the 4-th order in $t_{L,R}$
(Amplitude $\propto \Gamma^2$)
But: singular: $\propto \ln \frac{E_c}{T}$

$$\mathcal{H} = \sum_{k\sigma} \varepsilon_{k\sigma} \left(c^+_{kL\sigma} c_{kL\sigma} + c^+_{kR\sigma} c_{kR\sigma} \right) + \sum_{\sigma} \varepsilon_0 c^+_{0\sigma} c_{0\sigma} + U n_\uparrow n_\downarrow$$

$$+ \sum_{k\sigma} \left\{ \left(t_L c^+_{kL\sigma} + t_R c^+_{kR\sigma} \right) c_{0\sigma} + c^+_{0\sigma} \left(t_L^* c_{kL\sigma} + t_R^* c_{kR\sigma} \right) \right.$$

$$\varepsilon_0 \simeq E_c \cdot (\mathcal{N} - \mathcal{N}^*) ; \quad U \sim E_c ; \quad \Gamma_{L,R} = \pi \nu_{L,R} \cdot |t_{L,R}|^2$$

Mapping on the Anderson impurity model:

$$\left\{ \begin{matrix} \alpha_{k\sigma} \\ \beta_{k\sigma} \end{matrix} \right\} = u\, c_{kL\sigma} \pm v\, c_{kR\sigma} ; \qquad \left\{ \begin{matrix} u \\ v \end{matrix} \right\} = \frac{1}{\sqrt{|t_L|^2 + |t_R|^2}} \left\{ \begin{matrix} t_L \\ t_R \end{matrix} \right\}$$

Band $\alpha_{k\sigma}$: like in the "usual" Anderson imp. model

Band $\beta_{k\sigma}$: free electrons

L.G., Raikh 1988
Ng, Lee 1988

Kondo effect for an Anderson impurity in a bulk metal

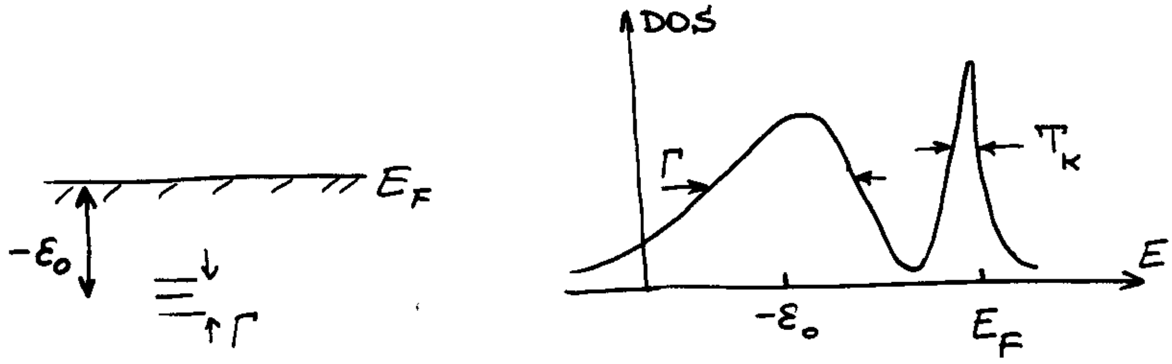

$$T_K \sim \sqrt{|\varepsilon_0|\Gamma}\, \exp\left\{-\frac{\pi|\varepsilon_0|}{\Gamma}\right\}$$ (Haldane 78)

Scattering is resonant at $T=0$ (L.G., Raikh 1988; Ng, Lee 1988)

$$\rho(T) = \rho_0 \cdot \underbrace{f\left(\frac{T}{T_K}\right)}_{\text{universal function}}$$

$f(x) = 1 - \pi^2 x^2, \; x \ll 1$ (Nozieres 74)

$f(0) = 1$: unitary limit

<u>Tunneling</u> through a dot: resonant at $T=0$

$$G(T) = \frac{e^2}{\pi\hbar} \cdot \frac{4\Gamma_l\Gamma_r}{(\Gamma_l+\Gamma_r)^2} \cdot f\left(\frac{T}{T_K}\right)$$

(L.G., Raikh 1988)

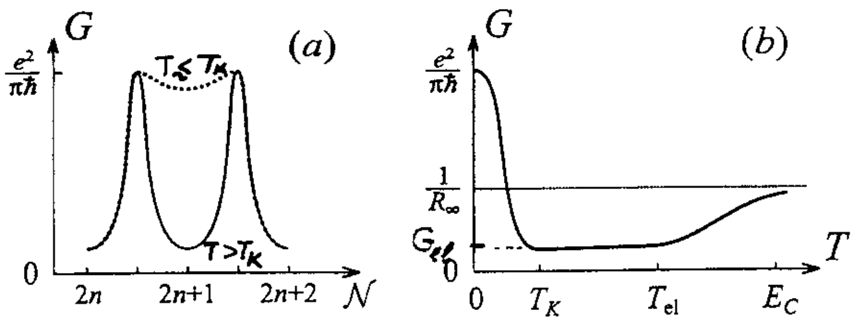

$$T_{el} \simeq \sqrt{E_c \cdot \delta E}$$

Conductance in an **odd** valley is non-monotonous

Difficulty # 1: Kondo temperature is very low:

$$T_K \sim \delta E \sqrt{\frac{\delta E}{E_c}} \sqrt{\frac{G_\ell + G_r}{e^2/\hbar}} \cdot \exp\Bigg\{-2\pi \underbrace{\frac{e^2/\hbar}{G_\ell + G_r}}_{\uparrow} \cdot \underbrace{\frac{E_c}{\delta E}}_{\uparrow} \cdot (N - N^*)\Bigg\}$$

Two large factors

Difficulty # 2: Kondo correction is very small above T_K:

$$\delta G_K \sim \underbrace{G_{el}} \cdot \frac{G_\ell + G_r}{e^2/\hbar} \left(\frac{\delta E}{E_c}\right)^2 \ln \frac{E_c}{T}$$

Background conductance
(elastic co-tunneling)

L.G., Hekking, Larkin: Proc. MB$\overline{\text{X}}$, 1999

What happens at <u>larger</u> conductance of the junction? $(\Gamma \to \delta E)$

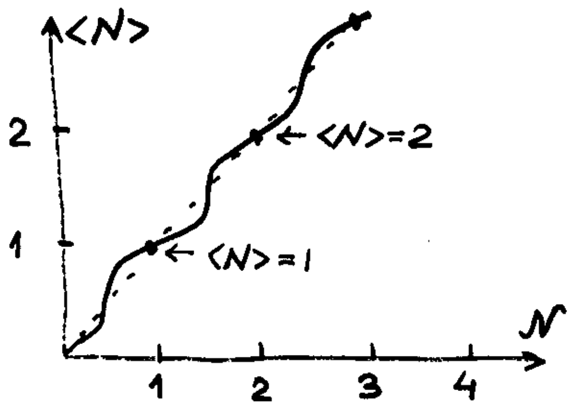

$\langle N \rangle \neq$ *integer*

Ⓢ ?

Model case:

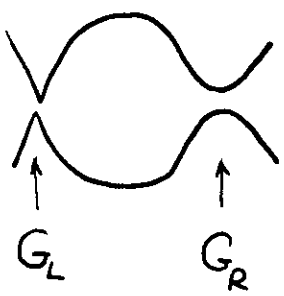

$$G_L \ll e^2/\pi\hbar$$

$$G_R = \frac{e^2}{\pi\hbar}\left(1 - |r|^2\right)$$

<u>r is small</u>

Mapping onto a 1D problem

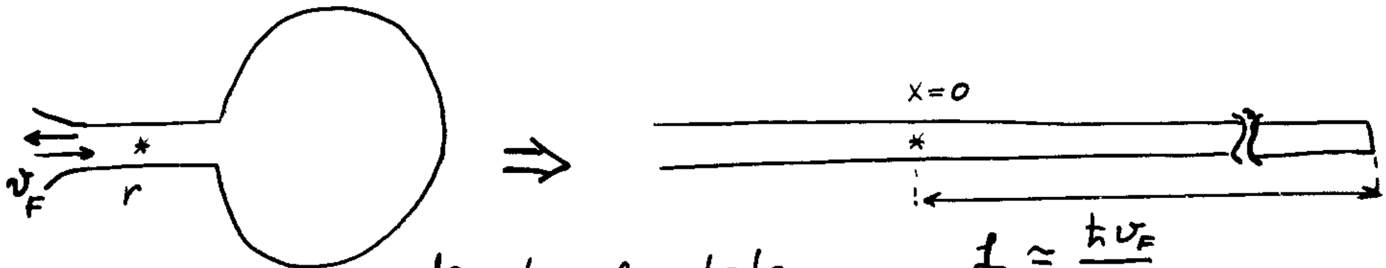

density of states in the dot $\sim \frac{1}{\delta E}$

$$\mathcal{H}_0 = i v_F \int_{-\infty}^{\mathcal{L}} dx \left\{ \psi^+_{L\sigma} \partial_x \psi_{L\sigma} - \psi^+_{R\sigma} \partial_x \psi_{R\sigma} \right\} +$$

$$+ E_c \left[\int_0^{\mathcal{L}} dx \left(:\psi^+_{L\sigma}\psi_{L\sigma} + \psi^+_{R\sigma}\psi_{R\sigma}: \right) - \mathcal{N} \right]^2$$

$$\mathcal{H}_{bs} = |r| v_F \left(\psi^+_{L\sigma}(0)\psi_{R\sigma}(0) + \psi^+_{R\sigma}(0)\psi_{L\sigma}(0) \right)$$

$r \leftrightarrow V(2k_F)$

(Matveev 95, $\mathcal{L} \to \infty$; Aleiner, L.G. 98, $\mathcal{L}$ finite)

Bosonized representation:

$$\psi^+_\sigma(x) = \hat{\eta}_\sigma \sqrt{\frac{D}{2\pi v_F}} \exp\left\{ i\sqrt{\frac{\pi}{2}} \left[\varphi_\rho(x) + \sigma \varphi_s(x) \right] \right\}$$

$$\times \exp\left\{ \pm i k_F x \pm i \sqrt{\frac{\pi}{2}} \left[\theta_\rho(x) + \sigma \theta_s(x) \right] \right\}$$

$\begin{pmatrix} + \to R \\ - \to L \end{pmatrix}$ $\qquad$ $[\nabla\varphi(x), \theta(y)] = -i\,\delta(x-y)$

$$\left.\begin{array}{l} \frac{2e}{\sqrt{\pi}} \nabla \theta_\rho(x) - \text{charge} \\ \frac{2}{\sqrt{\pi}} \nabla \theta_s(x) - \text{spin} \end{array}\right\} \text{densities}$$

$\sum_\sigma \psi_\sigma^+ \psi_\sigma \longrightarrow \partial_x \theta_\rho(x)$; $\hat{\mathcal{H}}_0$ becomes quadratic in the boson representation!

$$\mathcal{H}_0 = \frac{v_F}{2} \int_{-\infty}^{\mathcal{L}} dx \left[\frac{1}{2} (\partial_x \varphi_s)^2 + 2 (\partial_x \theta_s)^2 \right]$$

$$+ \frac{v_F}{2} \int_{-\infty}^{\mathcal{L}} dx \left[\frac{1}{2} (\partial_x \varphi_\rho)^2 + 2 (\partial_x \theta_\rho)^2 \right] + E_C \left[\frac{2}{\sqrt{\pi}} \theta_\rho(0) - N \right]^2$$

$$\mathcal{H}_{bs} = - \frac{2}{\pi} |r| \, D \cos(2\sqrt{\pi}\, \theta_\rho(0)) \cos(2\sqrt{\pi}\, \theta_s(0))$$

$$\theta_\rho(\mathcal{L}) = \theta_s(\mathcal{L}) = 0$$

Important energy scales:

E_C $\gg$	$E_C \lvert r \rvert^2$ $\gg$	$\delta E = \frac{\hbar v_F}{\mathcal{L}}$
(charging)	(effective barrier)	(level spacing)

In the absence of charging energy:

$\mathcal{H}_{bs}$ "counts" electrons:

$\mathcal{H}_{bs}$ is invariant under $\begin{cases} \theta_\rho \to \theta_\rho + \frac{\sqrt{\pi}}{2} \\ \theta_s \to \theta_s + \frac{\sqrt{\pi}}{2} \end{cases}$

In the presence of charging energy $E_c \left[\frac{2}{\sqrt{\pi}}\theta_\rho - \mathcal{N}\right]^2$:

charge mode is fixed,

$$\mathcal{H}_{bs} = -\frac{2}{\sqrt{\pi}} |r| D \cos(2\sqrt{\pi}\,\theta_\rho)\Big|_{\theta_\rho = \frac{\sqrt{\pi}}{2}\mathcal{N}} \cdot \cos(2\sqrt{\pi}\,\theta_s)$$

is invariant under $\theta_s \to \theta_s + \sqrt{\pi}$

and "counts" spins

Low energies: $\mathcal{H}_{bs}$ is relevant; $\mathcal{H}_{bs} \Rightarrow J_{eff.} \vec{S}_{dot} \cdot \vec{S}_{lead}$

1. Spin remains quantized, despite $\langle N \rangle \neq$ integer, as long as $|r|^2 \gtrsim \delta E / E_c$

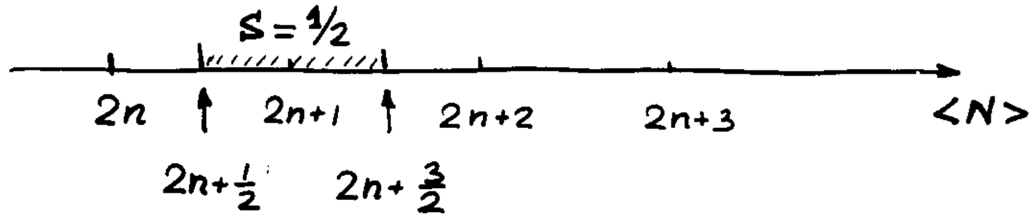

Kondo effect requires $\cos(\pi \langle N \rangle) < 0$

2. T_K is <u>enhanced</u>:

$$T_K \sim \delta E \cdot \exp\Big\{-2.26 \cdot \underbrace{\frac{E_c}{\delta E}}_{\text{large}} \cdot \underbrace{|r|^2}_{\text{small!}} \cdot \cos^2 \pi \mathcal{N} \cdot \overset{\text{random, }\sim 1}{\eta} \Big\}$$

3. $G_K(\mathcal{N}, T)$ is modified:

$$G_K\left(\mathcal{N}, \frac{T}{T_K}\right) \simeq G_L |r|^2 \cdot \cos^2(\pi \mathcal{N}) \cdot f\left(\frac{T}{T_K}\right)$$

(L.G., Hekking, Larkin, PRL <u>83</u>, 1830 (1999))

Conductance: overall T-dependence

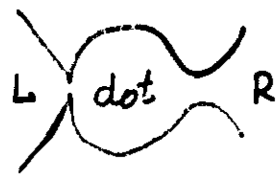

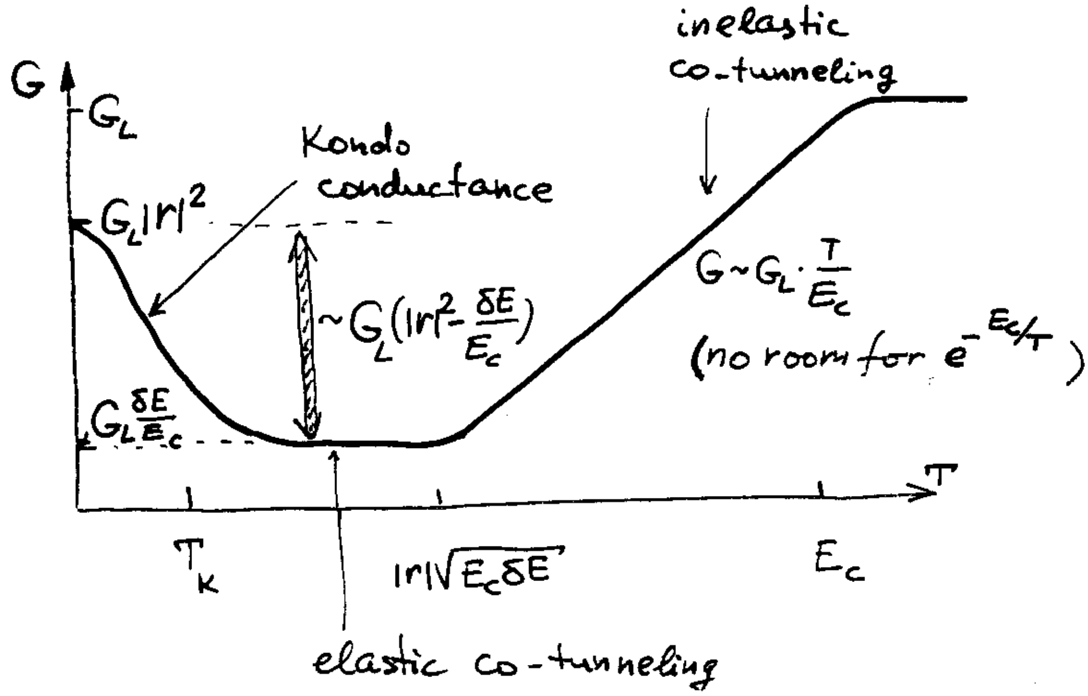

Dot spin is well-defined and Kondo persists, if

$$|r|^2 \gtrsim \frac{\delta E}{E_c}$$

Hamiltonian:

$$\mathcal{H} = \mathcal{H}_F + \mathcal{H}_{int}$$

Free quasiparticles:

$$\mathcal{H}_F = \sum_{\substack{\alpha,\beta \\ \sigma}} \mathcal{H}_{\alpha\beta} \psi^+_{\alpha\sigma} \psi_{\beta\sigma} \longrightarrow \sum_{n,\sigma} \xi_n a^+_{n\sigma} a_{n\sigma}$$

$P(\xi_{n+1} - \xi_n)$: Wigner-Dyson distribution of <u>orbital</u> energy spacings

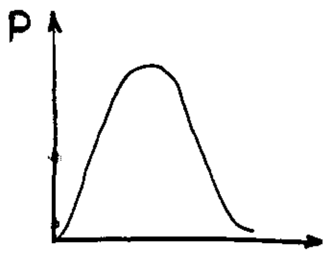

$\delta E = \xi_{n+1} - \xi_n$

Interaction:

$$\mathcal{H}_{int} = \mathcal{H}^{(0)}_{int} + \mathcal{H}^{(1)}_{int}$$

<u>small</u> fluctuations ($G \gg 1$)

<u>universal</u>

Altshuler et. al. 97
Agam et. al. 97
Blanter, Mirlin 97
Aleiner, L.G. 98

Coulomb blockade peak positions

"Universal" model ($r_s \ll 1$):

$$\mathcal{H} = \mathcal{H}_{\text{free}} + \mathcal{H}_{\text{int}}, \qquad \mathcal{H}_{\text{int}} = E_C(\hat{N} - \mathcal{N})^2;$$

$$\mathcal{H}_{\text{free}} = \sum_{n,\sigma} \xi_n a^\dagger_{n\sigma} a_{n\sigma}.$$

Bimodal distribution: each orbital level ξ_n accomodates two electrons with *opposite* spins

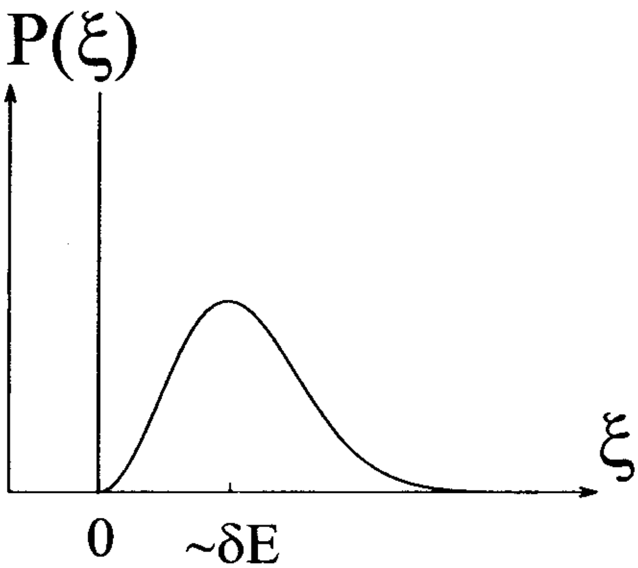

δ-peak: adding e to the same orbital level

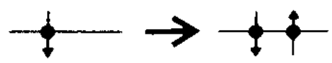

P_{WD}: Wigner-Dyson distribution for adding e to the next orbital level

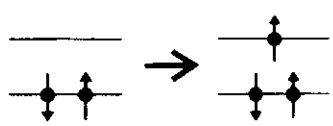

The universal part:

$$\mathcal{H}^{(0)}_{int} = E_c(\hat{N}-\mathcal{N})^2 - J_s(\vec{S})^2 + J_c \hat{T}^+\hat{T}$$

$$\hat{N} = \sum_{\alpha,\sigma} \psi^+_{\alpha\sigma}\psi_{\alpha\sigma} = \sum_{n,\sigma} a^+_{n\sigma}a_{n\sigma}$$ # of electrons

$$\hat{\vec{S}} = \frac{1}{2}\sum_{\substack{\alpha\\ \sigma_1,\sigma_2}} \psi^+_{\alpha\sigma_1}\vec{\sigma}_{\sigma_1\sigma_2}\psi_{\alpha\sigma_2}$$ total spin

$$\hat{T} = \sum_{\alpha} \psi_{\alpha\uparrow}\psi_{\alpha\downarrow}$$ "s/c operator"

Constant Interaction (CI) model:

$$\mathcal{H}_{CI} = \sum_{\substack{n\\ \sigma}} \xi_n a^+_{n\sigma}a_{n\sigma} + E_c(\hat{N}-\mathcal{N})^2 \;;$$

$J_c \to 0$, $J_s \to 0$, $\mathcal{H}^{(1)}_{int} \to 0$

Beyond CI:

$J_s \sim r_s \langle \delta E \rangle$; no macroscopic $\langle \vec{S} \rangle$ in the ground state (Stoner criterion)
(Kurland et. al. cond-mat/0004205)

If interaction $\mathcal{H}_{\alpha\alpha\gamma\gamma}$ is attractive, then $J_c \to -\langle \delta E \rangle$ in large grains ($\delta E \ll \Delta$)

Finite (but small) r_s:

shifts and reduces the amplitude of the δ-peak, but does not eliminate it.

(Brouwer, Oreg, Halperin cond-mat/9907148
Baranger, Ullmo, Glazman cond-mat/9907151
PRB 62, R2425, 2000)

* Andreev, Kamenev, PRL 81 3199 (1998)

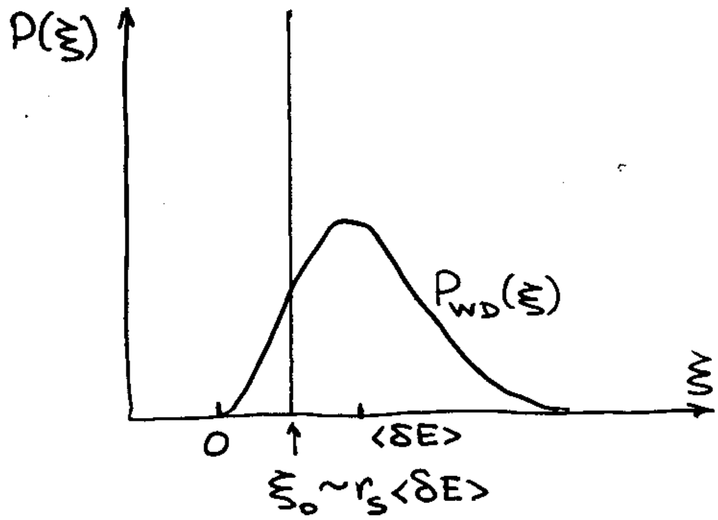

$$P(\xi) = \frac{1}{2}\left[(1-\alpha)\,\delta(\xi-\xi_0) + (1+\alpha)\,P_{WD}(\xi)\right]$$

broadens only at finite $\frac{h}{e^2}\sigma$
(dirty limit,

singlet → triplet

$r_s \langle \delta E \rangle > \delta E$

Signatures of spin pairing in a quantum dot in the Coulomb blockade regime

S. Lüscher[1], T. Heinzel[1], K. Ensslin[1], W. Wegscheider,[2,3] and M. Bichler[3]
[1] *Solid State Physics Laboratory, ETH Zürich, 8093 Zürich, Switzerland*
[2] *Institut für Angewandte und Experimentelle Physik, Universität Regensburg, 93040 Regensburg, Germany*
[3] *Walter Schottky Institut, TU München, 85748 Garching, Germany*
(February 15, 2000, cond-mat/0002226)

Coulomb blockade resonances are measured in a GaAs quantum dot in which both shape deformations and interactions are small. The parametric evolution of the Coulomb blockade peaks shows a pronounced pair correlation in both position and amplitude, which is interpreted as spin pairing. As a consequence, the nearest-neighbor distribution of peak spacings can be well approximated by a smeared bimodal Wigner surmise, provided that interactions which go beyond the constant interaction model are taken into account .

PACS numbers: 73.20.My, 73.23.Hk, 05.45.+b

$$P(s) = \frac{1}{2}\left[\delta(s) + P^{\beta}(s)\right] \tag{1}$$

$P^{\beta}(s)$ is the Wigner surmise for the corresponding Gaussian ensemble, i.e. $\beta = 1$ for systems with time inversion symmetry (Gaussian orthogonal ensemble - GOE), and $\beta = 2$ when time inversion symmetry is broken (Gaussian unitary ensemble - GUE). The peak spacing s is measured in units of the average spin-degenerate energy level spacing.

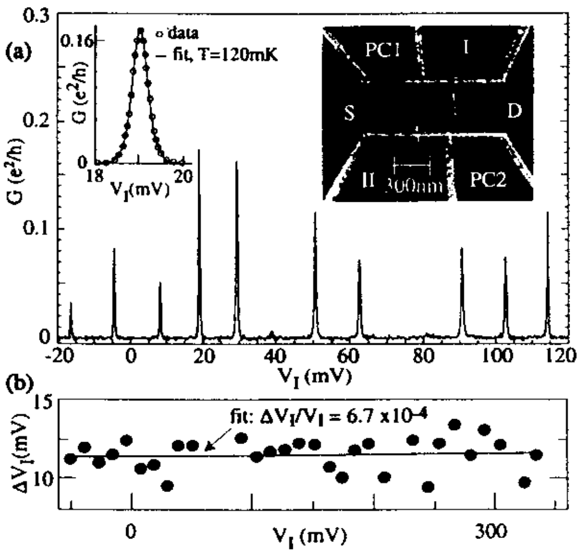

FIG. 1. (a) Right inset: AFM picture (taken before evaporation of the top gate) of the oxide lines (bright) that define the dot, coupled to source (S) and drain (D) via tunnel barriers, which can be adjusted with the planar gates PC1 and PC2. Gates I and II are used to tune the dot. Main figure: Conductance G as a function of V_I, showing Coulomb blockade resonances. Left inset: fit (line) to one measured CB peak (open circles), see text. (b) Linear fit (line) of the peak spacing ΔV_I as a function of V_I (dots). The average peak spacing is almost constant, indicating small shape deformations.

$$P^{\beta}_{int}(\overline{\xi^*}, \sigma_{\xi^*}) =$$
$$\frac{1}{\sqrt{2\pi}\sigma_{\xi^*}}\left\{exp\left[-\frac{(s-\overline{\xi^*})^2}{2\sigma^2_{\xi^*}}\right] + exp\left[-\frac{s^2}{2\sigma^2_{\xi^*}}\right] \times P^{\beta}(s+\xi^*)\right\} \tag{2}$$

Here, the "$\times$" denotes the convolution.

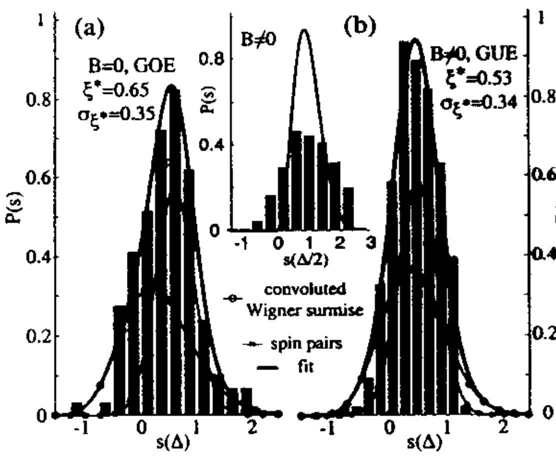

FIG. 2. Measured NNS distributions (gray bars) for B=0 (a) and B $\neq$ 0 (b). The bold solid curves are the fits to $P^{\beta}_{int}(\overline{\xi^*}, \sigma_{\xi^*})$, with the fit results as indicated in the figure (see text). Also drawn are the two components of P^{β}_{int}, i.e. the Gaussian distribution of separations between spin pairs, and its convolution with the corresponding Wigner surmises. The inset compares the GUE data to $P^2(s)$ (eq. 1), using the spin-resolved level spacing $\Delta/2$ as the average peak separation.

[1] For a review, see L.P. Kouwenhoven, C.M. Marcus, P.L. McEuen, S. Tarucha, R.M. Westervelt, and N.S.

38

Conclusions

1. The majority of experiments can be described by a <u>constant-interaction</u> model of a quantum dot

$$\mathcal{H} = \sum_n \xi_n a^+_{n\sigma} a_{n\sigma} + E_C (\hat{N} - N)^2$$

2. Crossover closed-open dot occurs at $G \sim e^2/\pi\hbar$

3. Most notable deviations from the constant-interaction model apparently are due to the <u>exchange</u> <u>interaction</u>

$$\mathcal{H}_{ex} = - r_s \langle \delta E \rangle \cdot \left[\vec{S}_{dot} \right]^2$$